Updating Kriging Surrogate Models Based on the Hypervolume Indicator in Multi-Objective Optimization

Koji Shimoyama[1]
Assistant Professor
Institute of Fluid Science,
Tohoku University,
Sendai 980-8577, Japan
e-mail: shimoyama@edge.ifs.tohoku.ac.jp

Koma Sato
Researcher
Hitachi Research Laboratory,
Hitachi, Ltd.,
Hitachinaka, Ibaraki 312-0034, Japan
e-mail: koma.sato.ky@hitachi.com

Shinkyu Jeong
Associate Professor
Department of Mechanical Engineering,
Kyunghee University,
Yongin 446-701, Korea
e-mail: icarus@khu.ac.kr

Shigeru Obayashi
Professor
Institute of Fluid Science,
Tohoku University,
Sendai 980-8577, Japan
e-mail: obayashi@ifs.tohoku.ac.jp

This paper presents a comparison of the criteria for updating the Kriging surrogate models in multi-objective optimization: expected improvement (EI), expected hypervolume improvement (EHVI), estimation (EST), and those in combination (EHVI + EST). EI has been conventionally used as the criterion considering the stochastic improvement of each objective function value individually, while EHVI has recently been proposed as the criterion considering the stochastic improvement of the front of nondominated solutions in multi-objective optimization. EST is the value of each objective function estimated nonstochastically by the Kriging model without considering its uncertainties. Numerical experiments were implemented in the welded beam design problem, and empirically showed that, in an unconstrained case, EHVI maintains a balance between accuracy, spread, and uniformity in nondominated solutions for Kriging-model-based multiobjective optimization. In addition, the present experiments suggested future investigation into techniques for handling constraints with uncertainties to enhance the capability of EHVI in constrained cases. [DOI: 10.1115/1.4024849]

1 Introduction

Surrogate models (or *metamodels*) are effective in reducing the computational time required in real-world design optimization. Surrogate models approximate the response of an objective or constraint function to design variables in the form of a simple algebraic function. This algebraic function is derived to interpolate the sample points with *real* values of the objective or constraint function given by expensive numerical simulation, and thus surrogate models can promptly give an *estimation* of function values at other points with unknown values of the function.

The most widely used surrogate model is the polynomial-based model [1]. This model strictly assumes *orthogonality* of the sample points given for the surrogate model construction. Thus, when the accuracy of the constructed surrogate model is insufficient, it is the easiest but most wasteful way to discard and regenerate the initial samples for a new surrogate model. Wang [2] proposed an adaptive polynomial-based model that can avoid discarding initial samples. However, it is very often difficult to set the order of polynomial so that the polynomial-based model will globally imitate the features of real functions in the whole design space. The radial basis function network (RBFN) [3] is an alternative surrogate model that permits any in-filling samples without satisfying those orthogonality. However, the RBFN does not provide any information about where in the design space these new sample points should be added.

This paper focuses on the Kriging surrogate model [4,5]. This model is based on Bayesian statistics, and can adapt well to nonlinear functions. Considering the approximation of a function $f(\boldsymbol{x})$ in terms of a design variable vector $\boldsymbol{x}$, as illustrated in Fig. 1, the Kriging model estimates not only the function value $\hat{f}(\boldsymbol{x})$ itself but also the *uncertainty* $\hat{s}(\boldsymbol{x})$ that is equivalent to the approximation error due to surrogate modeling (a full derivation of $\hat{f}(\boldsymbol{x})$ and $\hat{s}(\boldsymbol{x})$ is given in Ref. [4]). The stochastic features modeled by $\hat{f}(\boldsymbol{x})$ and $\hat{s}(\boldsymbol{x})$ help to determine the locations in the design space where new sample points should be added for improvement of surrogate model accuracy.

Jones et al. [5] proposed a practical approach to determine the locations of additional sample points, designated efficient global optimization (EGO). On the Kriging surrogate model, EGO searches for the location where the EI of an original objective function is maximized, and then reconstructs the surrogate model by adding a new sample point at this location. Consequently, iteration of this process will accomplish surrogate model accuracy improvements as well as the exploration of a global optimum. Then, Jeong et al. [6] proposed an extension of EGO for multi-objective problems (EGOMOP), which evaluates EI of each objective function and maximizes multiple EIs in terms of all objective functions. Li et al. [7] proposed another criterion to judge whether new sample points are needed based on the domination status in Kriging-based multiobjective optimization. Li [8] also improved this criterion to make the judgment more accurate and less influential to the uncertainty latent in the Kriging model. Martin [9] proposed an efficient formulation to construct the Kriging model construction by introducing gradient and Hessian terms into the maximum likelihood estimation. Moreover, the Kriging model has recently been contributing to a realization of challenging design optimization that had never been implemented before

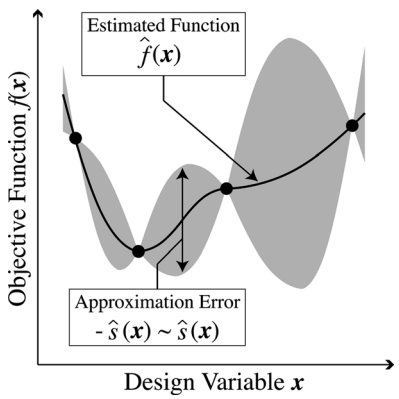

Fig. 1 Kriging model

[1]Corresponding author.

Contributed by the Design Automation Committee of ASME for publication in the JOURNAL OF MECHANICAL DESIGN. Manuscript received September 24, 2012; final manuscript received May 15, 2013; published online July 2, 2013. Assoc. Editor: Bernard Yannou.

due to insufficient computational resources, such as robust design [10] and reducible uncertain interval design [11]. Recent surrogate-model-based techniques and these related matters, which are not restricted within the Kriging model, were extensively reviewed by Wang and Shan [12].

With regard to the Kriging updating strategy, the EHVI [13] has also been proposed as an alternate criterion for updating the Kriging models generated in multiobjective optimization. EHVI focuses on improvement of the front of nondominated solutions in a multiobjective function space, while EI focuses on the improvement of each objective function value itself. Therefore, maximizing EHVI instead of EI is expected to achieve more efficient exploration of global optima in multi-objective problems. In addition, Emmerich et al. [14] confirmed the monotonicity of the EHVI criterion analytically for two-objective problems. However, there is no report that comprehensively inspects and compares the performance of different updating criteria (EI, EHVI, etc.) in several optimization cases with different features (e.g., existence of constraints).

This paper compares the criteria for updating Kriging surrogate models in multiobjective optimization: EI, EHVI, EST of an objective function itself, and those in combination. The current comparison is implemented through numerical experiments in the welded beam design problem, which includes both unconstrained and constrained cases. Thus, this paper investigates the capabilities of each criterion to search for nondominated solutions on the Kriging surrogate models in unconstrained and constrained multiobjective optimization comprehensively.

2 Criteria for Updating the Kriging Model

2.1 EI. EI is the expected value of how much an objective function $f(\boldsymbol{x})$ may be improved on the Kriging surrogate model, which will be reconstructed for $f(\boldsymbol{x})$ with the additional point $\boldsymbol{x}$. In a single-objective problem where $f(\boldsymbol{x})$ is minimized, as illustrated in Fig. 2(*a*), the function improvement $I[f(\boldsymbol{x})]$ and its expected value $\mathrm{EI}[f(\boldsymbol{x})]$ are expressed, respectively, as

$$I[f(\boldsymbol{x})] = \begin{cases} f_{\mathrm{ref}} - F & \text{if} \quad F < f_{\mathrm{ref}} \\ 0 & \text{otherwise} \end{cases} \tag{1}$$

$$\begin{aligned} \mathrm{EI}[f(\boldsymbol{x})] &= \int_{-\infty}^{\infty} I[f(\boldsymbol{x})]\phi(F)\mathrm{d}F \\ &= \int_{-\infty}^{f_{\mathrm{ref}}} (f_{\mathrm{ref}} - F)\phi(F)\mathrm{d}F \end{aligned} \tag{2}$$

where F is the Gaussian random variable $\mathrm{N}[\hat{f}(\boldsymbol{x}), \hat{s}^2(\boldsymbol{x})]$, and $\phi(F)$ is the probability density function of F, i.e., $\phi(F) = \exp\left[-\left(F - \hat{f}(\boldsymbol{x})\right)^2/(2\hat{s}^2(\boldsymbol{x}))\right]/\left(\sqrt{2\pi}\hat{s}(\boldsymbol{x})\right)$. In addition, f_{ref} is the reference value to be specified for evaluating the improvement $I[f(\boldsymbol{x})]$. Usually in a single-objective problem, the minimum value of $f(\boldsymbol{x})$ in the current dataset of sample points is considered as f_{ref}, as illustrated in Fig. 2(*a*), and the EI value corresponds to the probability that the Kriging predictor $\hat{f}(\boldsymbol{x})$ may achieve a new global optimum at $\boldsymbol{x}$ on the reconstructed surrogate model. In the concept of EI criterion, therefore, the location $\boldsymbol{x}$ with the maximum value of $\mathrm{EI}[f(\boldsymbol{x})]$ should be searched for as an additional sample point. Moreover, in a multi-objective problem where $f_1(\boldsymbol{x}), f_2(\boldsymbol{x}), \ldots, f_m(\boldsymbol{x})$ are minimized, EIs are evaluated and maximized for all the objective functions individually using Eq. (2), as $\mathrm{EI}[f_1(\boldsymbol{x})]$, $EI[f_2(\boldsymbol{x})], \ldots, \mathrm{EI}[f_m(\boldsymbol{x})]$.

2.2 EHVI. EHVI is based on the theory of the *hypervolume indicator* [15], which is a measure reflecting the quality of a set of nondominated solutions produced in multi-objective optimization. The hypervolume indicator consists of the size of the region fronted by the nondominated solutions and bounded above by a reference point. This study used an efficient algorithm for calculating the hypervolume indicator, as proposed previously [16].

Thus, EHVI is the expected value of how much the hypervolume indicator may be improved on the Kriging surrogate model, which will be reconstructed for $f_1(\boldsymbol{x}), f_2(\boldsymbol{x}), \ldots, f_m(\boldsymbol{x})$, respectively, with the additional point $\boldsymbol{x}$. The hypervolume improvement $\mathrm{HVI}[f_1(\boldsymbol{x}), f_2(\boldsymbol{x}), \ldots, f_m(\boldsymbol{x})]$ is defined as the hypervolume bounded above by the nondominated front of the current dataset of sample points, as illustrated in Fig. 2(*b*), and its expected value $\mathrm{EHVI}[f_1(\boldsymbol{x}), f_2(\boldsymbol{x}), \ldots, f_m(\boldsymbol{x})]$ is expressed as

$$\begin{aligned} &\mathrm{EHVI}[f_1(\boldsymbol{x}), f_2(\boldsymbol{x}), \ldots, f_m(\boldsymbol{x})] \\ &\quad = \int_{-\infty}^{f_{1\mathrm{ref}}} \int_{-\infty}^{f_{2\mathrm{ref}}} \cdots \int_{-\infty}^{f_{m\mathrm{ref}}} \mathrm{HVI}[f_1(\boldsymbol{x}), f_2(\boldsymbol{x}), \ldots, f_m(\boldsymbol{x})] \\ &\qquad \times \phi_1(F_1)\phi_2(F_2)\cdots\phi_m(F_m)\mathrm{d}F_1\mathrm{d}F_2\cdots\mathrm{d}F_m \end{aligned} \tag{3}$$

where $F_1, F_2, \ldots, F_m$ are the Gaussian random variables $\mathrm{N}[\hat{f}_1(\boldsymbol{x}), \hat{s}_1^2(\boldsymbol{x})], \mathrm{N}[\hat{f}_2(\boldsymbol{x}), \hat{s}_2^2(\boldsymbol{x})], \ldots, \mathrm{N}[\hat{f}_m(\boldsymbol{x}), \hat{s}_m^2(\boldsymbol{x})]$, respectively, $\phi_1(F_1), \phi_2(F_2), \ldots, \phi_m(F_m)$ are the probability density functions of $F_1, F_2, \ldots, F_m$, respectively, and $f_{1\mathrm{ref}}, f_{2\mathrm{ref}}, \ldots, f_{m\mathrm{ref}}$ are the reference values to be specified for evaluating the hypervolume improvement $\mathrm{HVI}[f_1(\boldsymbol{x}), f_2(\boldsymbol{x}), \ldots, f_m(\boldsymbol{x})]$. The EHVI value corresponds to the probability that a combination of the Kriging predictors $\hat{f}_1(\boldsymbol{x}), \hat{f}_2(\boldsymbol{x}), \ldots, \hat{f}_m(\boldsymbol{x})$ may achieve a new nondominated solution at $\boldsymbol{x}$ on the reconstructed surrogate model. Similar to the EI criterion, therefore, the concept of EHVI criterion indicates that the search should be conducted for location $\boldsymbol{x}$ with the maximum value of $\mathrm{EHVI}[f(\boldsymbol{x})]$ as an additional sample point.

2.3 EST. For a comparison with EI and EHVI, EST is also considered here. EST is the value of an objective function $f(\boldsymbol{x})$, which is estimated nonstochastically by the Kriging model without considering its uncertainties, i.e., $\hat{f}(\boldsymbol{x})$ itself. In the concept of EST criterion, a straightforward search is performed for the

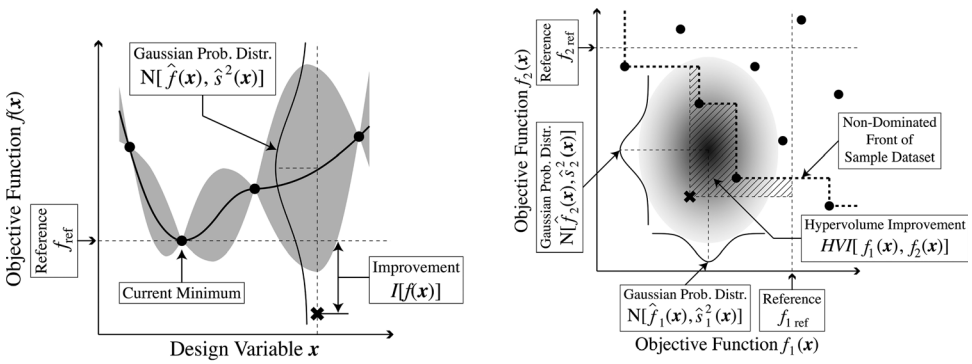

Fig. 2 Criteria for updating the Kriging model: (*a*) EI and (*b*) EHVI

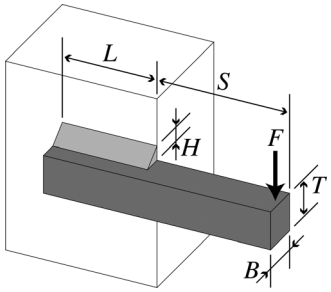

Fig. 3 Welded beam design problem

location of $\boldsymbol{x}$ with the minimum value of $\hat{f}(\boldsymbol{x})$ as an additional sample point. It is only natural that this concept may lead to an incorrect global optimal due to ignorance regarding surrogate model approximation error $\hat{s}(\boldsymbol{x})$.

3 Numerical Experiments

3.1 Problem Definition. This paper performed numerical experiments in the multiobjective welded beam design problem, as illustrated in Fig. 3, which minimizes

$$f_1(\boldsymbol{x}) = \text{Disp} \tag{4a}$$

$$f_2(\boldsymbol{x}) = \text{Cost} \tag{4b}$$

subject to

$$g_1(\boldsymbol{x}) = H - B \le 0 \tag{5a}$$

$$g_2(\boldsymbol{x}) = \text{Max}S - 60 \le 0 \tag{5b}$$

$$g_3(\boldsymbol{x}) = \text{Max}T - 100 \le 0 \tag{5c}$$

where

$$\text{Disp} = \frac{F \times S^3}{4 \times T^3 \times B \times \text{Young}} \quad \text{(beam tip displacement)}$$

$$\text{Cost} = W_c \times W_{\text{vol}} + M_c \times M_{\text{vol}} \quad \text{(total cost)}$$

$$W_{\text{vol}} = H^2 \times L \quad \text{(weld volume)}$$

$$M_{\text{vol}} = T \times B \times (S + L) \quad \text{(beam volume)}$$

$$\text{Max}S = \sqrt{t1^2 + t2^2} \quad \text{(maximum shear stress)}$$

$$\text{Max}T = \frac{6 \times S \times F}{T^2 \times B} \quad \text{(maximum tensional stress)}$$

$$t1 = \frac{F(S + L/2)}{B \times \text{Area}}$$

$$t2 = \frac{F}{2 \times \text{Area}}$$

$$\text{Area} = L \times H \times \sqrt{2}$$

Fixed parameters are $M_c = 0.01$ (beam cost per unit volume), $W_c = 1$ (weld cost per unit volume), Young = 250,000 (Young's modulus), $F = 150$ (beam tip load), and $S = 100$ (beam length). The other parameters are the design variables, $\boldsymbol{x} = [x_1, x_2, x_3, x_4]^{\mathrm{T}} = [H, L, T, B]^{\mathrm{T}}$, whose ranges are set as $1 \le H \le 15$ (weld height), $3 \le L \le 50$ (weld length), $10 \le T \le 50$ (beam height), and $1 \le B \le 15$ (beam width), respectively.

3.2 Test Cases. Four Kriging models were constructed for two objective functions $f_1(\boldsymbol{x})$ and $f_2(\boldsymbol{x})$ (Eqs. 4(*a*) and 4(*b*)) and two constraint functions $g_2(\boldsymbol{x})$ and $g_3(\boldsymbol{x})$ (Eqs. 5(*b*) and 5(*c*)), while the remaining constraint function $g_1(\boldsymbol{x})$ (Eq. 5(*a*)) was not approximated by the Kriging model. Note that $g_1(\boldsymbol{x}) \le 0$ determines the order of size between two design variables H and B, and can always be satisfied in a subordinate procedure without expensive function evaluation, e.g., first specifying a value for H and then specifying a larger value for B.

These experiments compare the following four different criteria for updating Kriging models in the welded beam design problem, each of which is formulated as

EST:

$$\begin{aligned} &\text{Minimize} : \hat{f}_1(\boldsymbol{x}) \\ &\text{Minimize} : \hat{f}_2(\boldsymbol{x}) \\ &\text{Subject to} : \hat{\boldsymbol{g}}(\boldsymbol{x}) \le \boldsymbol{0} \end{aligned}$$

EI:

$$\begin{aligned} &\text{Maximize} : \text{EI}[f_1(\boldsymbol{x})] \times Pn(\boldsymbol{x}) \\ &\text{Maximize} : \text{EI}[f_2(\boldsymbol{x})] \times Pn(\boldsymbol{x}) \end{aligned}$$

EHVI:

$$\text{Maximize} : \text{EHVI}[f_1(\boldsymbol{x}), f_2(\boldsymbol{x})] \times Pn(\boldsymbol{x})$$

EHVI + EST:

$$\begin{aligned} &\text{Minimize} : \hat{f}_1(\boldsymbol{x}) \\ &\text{Minimize} : \hat{f}_2(\boldsymbol{x}) \\ &\text{Maximize} : EHVI[f_1(\boldsymbol{x}), f_2(\boldsymbol{x})] \times Pn(\boldsymbol{x}) \end{aligned}$$

in the following two problems with different combinations of constraints, each of which results in a different penalty function $Pn(\boldsymbol{x})$ as

Problem 1: Considering $g_1(\boldsymbol{x}) \le 0$ only (equivalent to an unconstrained problem)

$$Pn(\boldsymbol{x}) = 1$$

Problem 2: Considering all the constraints

$$Pn(\boldsymbol{x}) = \text{Prob}[g_2(\boldsymbol{x}) \le 0] \times \text{Prob}[g_3(\boldsymbol{x}) \le 0]$$

$\text{Prob}[g_2(\boldsymbol{x}) \le 0]$ and $\text{Prob}[g_3(\boldsymbol{x}) \le 0]$ are calculated from the stochastic features of the Kriging models as follows; considering a

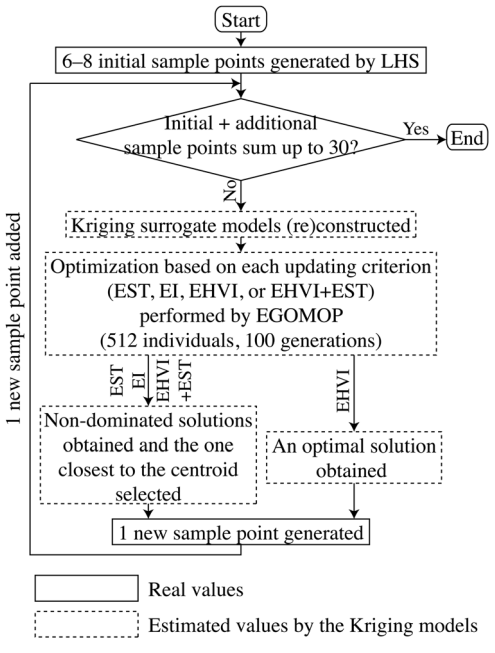

Fig. 4 Flowchart of updating the Kriging models

constraint function $g(\boldsymbol{x})$ approximated as $\hat{g}(\boldsymbol{x})$ with its approximation error $\hat{t}(\boldsymbol{x})$ (equivalent to an objective function $f(\boldsymbol{x})$ approximated as $\hat{f}(\boldsymbol{x})$ with its approximation error $\hat{s}(\boldsymbol{x})$),

$$\text{Prob}[g(\boldsymbol{x}) \le 0] = \int_{-\infty}^{0} \gamma(G)\mathrm{d}G \tag{6}$$

where G is the Gaussian random variable $\mathrm{N}[\hat{g}(\boldsymbol{x}), \hat{t}^2(\boldsymbol{x})]$, and $\gamma(G)$ is the probability density function of G, i.e., $\gamma(G) = \exp[-(G-\hat{g}(\boldsymbol{x}))^2/(2\hat{t}^2(\boldsymbol{x}))]/\left(\sqrt{2\pi}\hat{t}(\boldsymbol{x})\right)$. The reference values used for evaluating EI and EHVI are set as $f_{1\text{ref}} = 0.005$ and $f_{2\text{ref}} = 1,000$.

3.3 Numerical Settings. Figure 4 shows the flowchart of updating the Kriging models in the present numerical experiments. Each test case consists of 30 trials, each of which starts from a different initial dataset of sample points. The initial sample points are generated uniformly in the design variable space by Latin hypercube sampling (LHS) [17]. The number of initial sample points changes from 6 to 8 depending on the trials due to the satisfaction of $g_1(\boldsymbol{x}) \le 0$ in the LHS process.

On the Kriging models constructed from the initial sample points, the locations of additional sample points are determined using the EGOMOP software based on the formulations for each test case as outlined in Sec. 3.2. The EGOMOP employs a real-coded multi-objective genetic algorithm (512 individuals, 100 generations, Pareto ranking + fitness sharing for fitness assignment, stochastic universal sampling for parent selection, simulated binary crossover + polynomial mutation (10% rate) for offspring reproduction) with range adaptation to accelerate convergence toward the Pareto-optimal front while keeping search diversity, and all function evaluations are surrogated by the Kriging models. Indeed, EGOMOP has been demonstrated through several applications to real-world design problems where expensive numerical simulations must be conducted for function evaluation (e.g., Refs. [18,19]), and succeed in finding better design candidates than the baseline design in terms of all objective functions within realistic computational times.

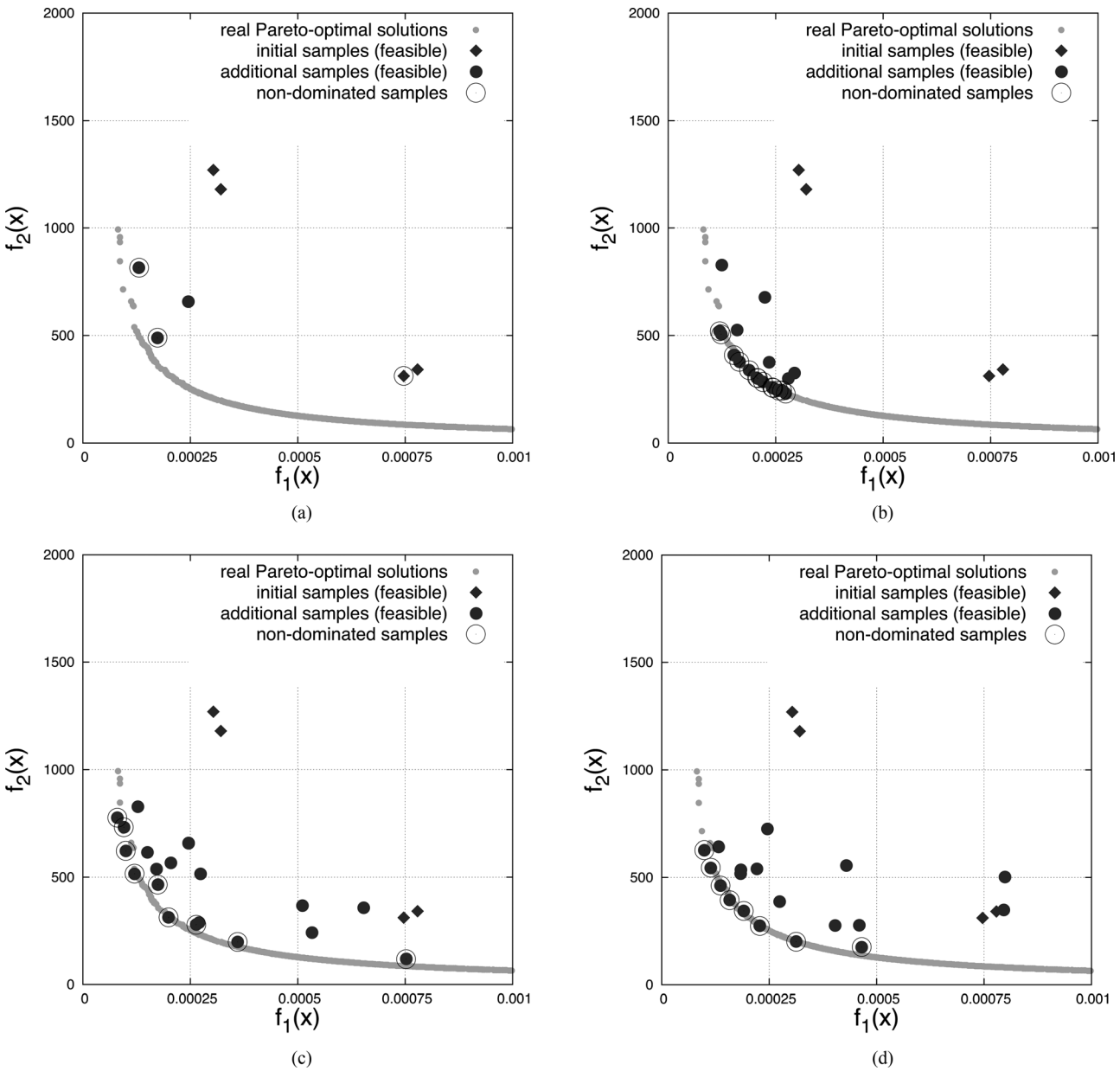

Fig. 5 Scatter plots of the sample points in objective function space obtained on the first trial in problem 1: (*a*) EST, (*b*) EI, (*c*) EHVI, and (*d*) EHVI + EST

Table 1 Comparison of the performance measures in problem 1 (nonbracketed value: mean, bracketed value: standard deviation evaluated for 30 trials)

	GD ($\times 10^{-3}$)	Spacing ($\times 10^{-2}$)	Spread ($\times 10^{-1}$)	Coverage ($\times 10^{-1}$)
EST	117.67 (143.66)	6.6683 (8.0840)	4.5170 (2.9370)	5.3662 (2.1372)
EI	7.3157 (7.8157)	6.3924 (4.0233)	5.8558 (1.7700)	8.7729 (0.46180)
EHVI	15.692 (10.427)	5.6148 (2.9240)	8.4935 (1.0171)	9.0999 (0.58333)
EHVI + EST	15.045 (11.681)	7.0262 (3.3214)	7.6221 (1.7585)	8.5991 (0.88021)

In the cases based on multi-objective formulations (EST, EI, and EHVI + EST), a set of nondominated solutions are obtained, and the solution closest to the centroid of all the solutions is selected as an additional sample point. In the case based on single-objective formulation (EHVI); on the other hand, a single optimal solution is obtained and employed as an additional sample point. This means that sample points are added one by one in all cases for a fair comparison. Then, the Kriging models are reconstructed and the search for the next additional sample point is performed. The update process of the Kriging models is iterated until the number of initial and additional sample points sums to 30.

3.4 Performance Measures. The Kriging model should lead to accurate estimation in a particular region to be interested in. In multi-objective optimization, this region corresponds to the neighborhood of Pareto-optimal front. Therefore, this paper considers all the following four measures important to investigate the performance, such that the real Pareto-optimal front can be captured

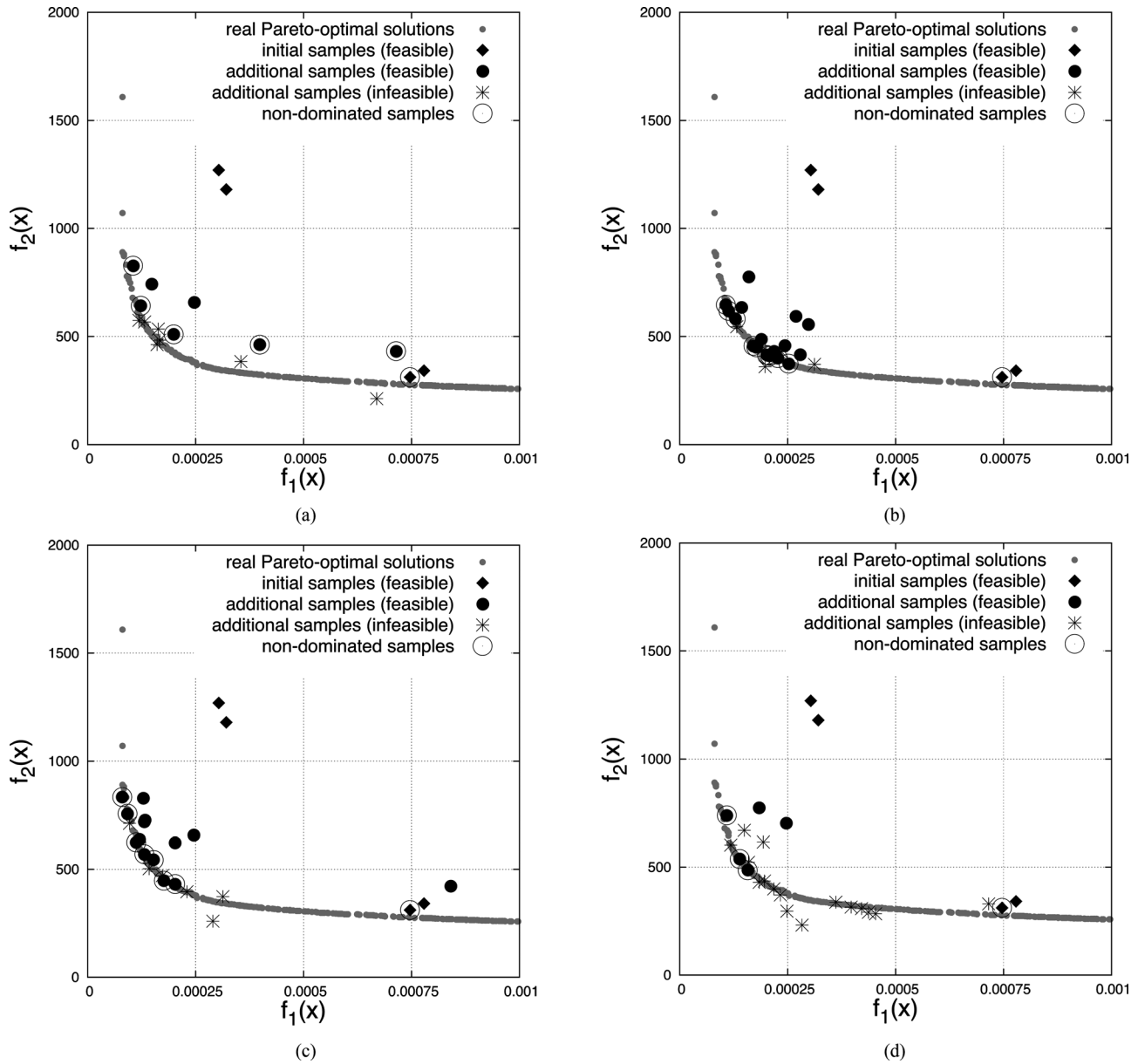

Fig. 6 Scatter plots of the sample points in objective function space obtained on the first trial in problem 2: (*a*) EST, (*b*) EI, (*c*) EHVI, and (*d*) EHVI + EST

Table 2 Comparison of the performance measures in problem 2 (nonbracketed value: mean, bracketed value: standard deviation evaluated for 30 trials)

	GD ($\times 10^{-3}$)	Spacing ($\times 10^{-2}$)	Spread ($\times 10^{-1}$)	Coverage ($\times 10^{-1}$)
EST	113.55 (125.98)	3.8440 (4.6441)	2.6607 (2.4889)	4.8707 (1.9933)
EI	11.555 (8.7630)	4.7448 (3.0115)	4.7234 (1.1748)	8.5923 (0.45371)
EHVI	16.403 (14.601)	6.7533 (4.9610)	6.0423 (1.2920)	8.3412 (0.62964)
EHVI + EST	41.375 (48.556)	7.4960 (6.7591)	4.0427 (2.3509)	7.0969 (1.3261)

by a finite number of nondominated solutions found on the Kriging models through different updating strategies. *Generational distance* (GD) [20] represents the proximity from the obtained nondominated solutions to the real Pareto-optimal front. *Spacing* [21] represents the uniformity of the obtained nondominated solutions. *Spread* [22] represents the extent of spread among the obtained nondominated solutions. *Coverage* [23] is defined as the ratio of a hypervolume dominated by the obtained nondominated solutions to that dominated by the real Pareto-optimal front, and represents the overall performance related to both proximity and spread. A smaller value is better in GD and Spacing, while a larger value is better in Spread and Coverage.

3.5 Results and Discussion

3.5.1 Problem 1. Figure 5 presents a comparison of scatter plots of the sample points in the objective function space, which were obtained on the first trial in problem 1, among four different criteria. Based on any criterion, the present experiments obtained additional samples, which are better than the initial samples in terms of $f_1(\boldsymbol{x})$ and $f_2(\boldsymbol{x})$. However, EST resulted in a much smaller number of nondominated samples than the other criteria, and these samples did not reach the real Pareto-optimal front due to surrogate model approximation error. On the other hand, EI resulted in many nondominated samples, which reach the real Pareto-optimal front, but these samples are concentrated on part of the front. EHVI and EHVI + EST resulted in several nondominated samples, although less than EI, and these samples are distributed widely on the real Pareto-optimal front (not only in the objective function space but also in the design variable space).

Table 1 presents a comparison of the performance measures among four different criteria in problem 1. The nonbracketed and bracketed values in each cell of Table 1 represent the mean and standard deviation of performance measure, respectively, which were statistically evaluated for 30 trials. EI showed the best average performance of GD and was followed by EHVI + EST and EHVI, while EST showed quite poor performance. On the other hand, EHVI showed the best average performance of Spacing and Spread. With regard to the overall performance measure Coverage, EHVI overwhelmed the other criteria. These results indicate that EHVI can maintain a balance between accuracy, spread, and uniformity in nondominated solutions for Kriging-model-based multi-objective optimization. Moreover, note that EST showed the largest standard deviation for all criteria, i.e., the capability of EST depends strongly on the choice of initial samples.

3.5.2 Problem 2. In problem 2, the scatter plots of the obtained sample points in the objective function space and the comparison of the evaluated performance measures are shown in Fig. 6 and Table 2, respectively. Note that problem 2 allows infeasible samples to be added because $g_2(\boldsymbol{x})$ and $g_3(\boldsymbol{x})$ were evaluated approximately by the Kriging models. In problem 2, not only EST but also EHVI + EST showed poor performance because most of the additional samples were infeasible, as shown in Figs. 6(*a*) and 6(*d*). On the other hand, EI and EHVI resulted in nondominated sample distributions (Figs. 6(*b*) and 6(*c*)). Table 2 indicates that EI is better than EHVI in terms of GD, Spacing, and Coverage, while EHVI is better than EI in terms of Spread. This means that EHVI did not overwhelm EI as much in problem 2 as in problem 1. Table 2 also implies that EST and EHVI + EST had large standard deviation for most criteria, i.e., the capabilities of EST and EHVI + EST are strongly dependent on the choice of initial samples. The differences in the numerical results between problems 1 and 2 were mainly due to poor accuracy of the Kriging model for $g_2(\boldsymbol{x})$. To enhance the capability of EHVI, the constraints with uncertainties should be handled in a more suitable way.

4 Conclusions

This paper described investigation and comparison of the capabilities of the criteria, EI, EHVI, EST, and those in combination (EHVI + EST), to search for nondominated solutions in the Kriging surrogate models in multi-objective optimization. Numerical experiments were implemented in the welded beam design problem. The numerical results in an unconstrained case empirically showed that although EI has good performance, particularly in terms of the proximity to a real Pareto-optimal front, EHVI maintains a balance between accuracy, spread, and uniformity in nondominated solutions for Kriging-model-based multi-objective optimization. However, the numerical results in a constrained case did not lead to such balanced performance for EHVI. As future work, therefore, a more sophisticated technique for handling constraints with uncertainties must be considered and tested to further enhance the capability of EHVI.

In addition, this paper considered only the welded beam design problem as the numerical experiments. In future, therefore, additional experiments need to be implemented in different problems with more objective functions to assure the generality of the present conclusions. However, the EHVI-based updating strategy may become impractical due to the fact that conventional algorithms to calculate the hypervolume indicator increase those computational time drastically as the number of objective functions increases. Thus, it is also essential to employ new efficient algorithms (e.g., Ref. [24]) for hypervolume calculation.

References

[1] Myers, R. H., and Montgomery, D. C., 1995, *Response Surface Methodology: Process and Product Optimization Using Designed Experiments*, Wiley, New York.
[2] Wang, G. G., 2003, "Adaptive Response Surface Method Using Inherited Latin Hypercube Design Points," ASME J. Mech. Des., **125**(2), pp. 210–220.
[3] Bishop, C. M., 1995, *Neural Networks for Pattern Recognition*, Oxford University, Oxford.
[4] Sacks, J., Welch, W. J., Mitchell, T. J., and Wynn, H. P., 1989, "Design and Analysis of Computer Experiments," Statist. Sci., **4**(4), pp. 409–435.
[5] Jones, D. R., Schonlau, M., and Welch, W. J., 1998, "Efficient Global Optimization of Expensive Black-Box Function," J. Global Optim., **13**, pp. 455–492.
[6] Jeong, S., Minemura, Y., and Obayashi, S., 2006, "Optimization of Combustion Chamber for Diesel Engine Using Kriging Model," J. Fluid Sci. Technol., **1**(2), pp. 138–146.
[7] Li, M., Li, G., and Azarm, S., 2008, "A Kriging Metamodel Assisted Multi-Objective Genetic Algorithm for Design Optimization," ASME J. Mech. Des., **130**(3), p. 031401.
[8] Li, M., 2011, "An Improved Kriging-Assisted Multi-Objective Genetic Algorithm," ASME J. Mech. Des., **133**(7), p. 071008.
[9] Martin, J. D., 2009, "Computational Improvements to Estimating Kriging Metamodel Parameters," ASME J. Mech. Des., **131**(8), p. 084501.
[10] Shimoyama, K., Lim, J. N., Jeong, S., Obayashi, S., and Koishi, M., 2009, "Practical Implementation of Robust Design Assisted by Response Surface Approximation and Visual Data-Mining," ASME J. Mech. Des., **131**(6), p. 0610071.
[11] Hamel, J. M., and Azarm, S., 2011, "Reducible Uncertain Interval Design by Kriging Metamodel Assisted Multi-Objective Optimization," ASME J. Mech. Des., **133**(1), p. 011002.
[12] Wang, G. G., and Shan, S., 2007, "Review of Metamodeling Techniques in Support of Engineering Design Optimization," ASME J. Mech. Des., **129**(4), pp. 370–380.

[13] Łaniewski-Wołłk, Ł., Obayashi, S., and Jeong, S., 2010, "Development of Expected Improvement for Multi-Objective Problem," Proceedings of 42nd Fluid Dynamics Conference/Aerospace Numerical Simulation Symposium 2010.
[14] Emmerich, M. T. M., Deutz, A. H., and Klinkenberg, J. W., 2011, "Hypervolume-Based Expected Improvement: Monotonicity Properties and Exact Computation," Proceedings of the 2011 IEEE Congress on Evolutionary Computation, IEEE Press, pp. 2147–2154.
[15] Zitzler, E., and Thiele, L., 1998, "Multiobjective Optimization Using Evolutionary Algorithms—A Comparative Case Study," Proceedings of the 5th International Conference on Parallel Problem Solving From Nature, Springer-Verlag, pp. 292–301.
[16] Beume, N., Fonseca, C. M., López-Ibáñez, M., Paquete, L., and Vahrenhold, J., 2009, "On the Complexity of Computing the Hypervolume Indicator," IEEE Trans. Evol. Comput., **13**(5), pp. 1075–1082.
[17] McKay, M. D., Beckman, R. J., and Conover, W. J., 1979, "A Comparison of Three Methods for Selecting Values of Input Variables in the Analysis of Output From a Computer Code," Technometrics, **21**(2), pp. 239–245.
[18] Sato, K., Kumano, T., Yonezawa, M., Yamashita, H., Jeong, S., and Obayashi, S., 2008, "Low-Boom and Low-Drag Optimization of the Twin Engine Version of Silent Supersonic Business Jet," J. Fluid Sci. Technol., **3**(4), pp. 576–585.
[19] Shimoyama, K., Yoshimizu, S., Jeong, S., Obayashi, S., and Yokono, Y., 2011, "Multi-Objective Design Optimization for a Steam Turbine Stator Blade Using LES and GA," J. Comput. Sci. Technol., **5**(3), pp. 134–147.
[20] Van Veldhuizen, D. A., and Lamont, G. B., 1998, "Multiobjective Evolutionary Algorithm Research: A History and Analysis, Air Force Institute of Technology, Dayton, OH, Technical Report No. TR–98–03.
[21] Schott, J. R., 1998, "Fault Tolerant Design Using Single and Multicriteria Genetic Algorithm Optimization," Master's thesis, Massachusetts Institute of Technology, Cambridge, MA.
[22] Zitzler, E., 1999, "Evolutionary Algorithms for Multiobjective Optimization: Methods and Applications," Ph.D. thesis, Swiss Federal Institute of Technology Zürich, Zürich, Switzerland.
[23] Van Veldhuizen, D. A., 1999, "Multiobjective Evolutionary Algorithms: Classifications, Analyses, and New Innovations," Ph.D. thesis, Air Force Institute of Technology, Dayton, OH.
[24] While, L., and Bradstreet, L., 2012, "Applying the WFG Algorithm to Calculate Incremental Hypervolumes," Proceedings of the 2012 IEEE Congress on Evolutionary Computation, IEEE Press, pp. 489–496.